PROFILES OF THE *H* AND *K* Ca II EMISSION REVERSALS IN SUNSPOTS

R. B. TEPLITSKAYA and S. A. EFENDEVA

SibIZMIRAN, Irkutsk, U.S.S.R.

Abstract: The profiles of K and H Ca II lines in the umbra and the penumbra of some spots locating near the solar disk centre are measured. In contrast to the results received by other authors the influence of a scattered light in the atmosphere and in the instrument is taken into account. The scattered light distores residual intensities of K- and H-emission reversals in the umbra more than in the case of usual absorption lines. The main typical feature of K- and H-lines in the umbra is an enormously high residual intensity of emission peaks. It changes from sunspot to sunspot and from point to point within the same umbra considerably, but it always exceeds 1 for large spots. The ratio of central residual intensities of the both multiplet lines is measured. The ratio $r_{(K3)}/r_{(H3)}$ is considerably more in the umbra of all the spots that in the penumbra and in surrounding plages. An average value is equal 1.20 ± 0.06. The profiles of K and H emission reversals are not similar to each other.

The way of determination of Doppler widths $\Delta\lambda_D$ of emission peaks is discussed. In the frames of accepted assumption about $\Delta\lambda_D$ behaviour a reverse problem is solved that means the K and H source function runs are calculated in the chromosphere about the sunspot.

Introduction

H and K resonance lines of ionized calcium are the subjects of a careful study of the solar spectrum. Rather accurate information about the profiles of these lines is available for quiet regions (e.g., White and Suemoto, 1968; Linsky, 1970) and for plages (Smith, 1960). High spatial resolution photographs show a large spatial and time variation of H and K. Nevertheless, the use of spectrographs with low spatial resolutions, or special approaches, providing averages over a broad part of the solar surface, allow one to obtain quite definite results, stable in time.

The problem of the H- and K-lines in sunspots is quite different. Even on photographs with a small resolution we can see a typical extraordinary variety of the form of central reversals, both inside one sunspot and when the different sunspots are compared. Perhaps, this is one of the reasons why mostly qualitative characteristics are known for sunspots and the quantitative data one emission reversal profiles are less numerous. Due to the lack of information about the chromosphere above the sunspots, a detailed study of the central parts of the H- and K-lines seems rather useful.

The present paper is based on the spectral data obtained at the Sayan Solar Observatory of SibIZMIR during 1968—1971 with an ACU-5 telescope and an ASP-2 spectrograph.

To reduce the variety of H- and K-profiles to a minimum, we have only chosen those sunspots which were located near the disk centre and examined the narrowly localized parts of each sunspot — a region of the umbra in the vicinity of the intensity minimum and the middle of the penumbra.

For strict photometric treatment of the H- and K-lines photo-electric measurements with a spectrograph with double passage are most suitable, since these instruments are free of proper scattered light and "ghosts" of the grating. These in particular are the best measurements of Ca II for the quiet Sun. However, this method is only suitable when simultaneous records of both lines can be obtained. For sunspots whose photometry is strongly affected by changes of the observational conditions, a photo-electric method seems to be less suitable than a photographic. Beside, the spectra of the umbra, the penumbra and the surrounding region are immediately seen on the photographs, which is important in reducing the profiles in the umbra. Using photographic observations, we tried in each case to check them with the help of standards, for which the photo-electric quiet chromosphere measurements, known from references, were chosen.

A great deal of attention was paid to the elimination of the scattered light effects of atmospheric and instrumental origin. Residual intensities of the H- and K-lines in the sunspot spectrum are affected by the presence of stray light even more than the profiles of other Fraunhofer lines. Usually this is neglected, because the central parts of the H- and K-lines are bright emission formations. However, one should not forget the distorted intensities of the continuum.

The profiles of the emission reversals in the H- and K-lines, obtained by photometric analysis, are used to study the source function in the chromosphere sunspot layers.

Observational Data

Spectrograms of sunspots are obtained in the VI order with the "ORWO Blue Hard" emulsion. Though this emulsion requires a rather long exposure time (3—4 sec for an umbra), it is convenient, because it exhibits the details of the central reversals with a high contrast. Each 13×18 cm^2 plate contains both lines of the Ca II doublet. At a dispersion of 3.60 mm/Å this location of lines eliminates the possibility of direct calibration against the "window" of the true continuum at 4000 Å. Therefore, the calibration was carried out with respect to the local continuum at 3954 Å.

According to Houtgast (1970), the intensity of the continuum "window" at 3954.2 Å, r_{3954}, is 83.6% of the true continuum intensity near 4000 Å. This value is conserved in plages too (Shine and Linsky, 1972). To be able to judge what r_{3954} is in sunspots, we have carried out photometric tracking across the dispersion direction in λ 3954.2 Å and in λ 4000 Å. Additional plates of sunspots, photographed in the II order, were used. Within measurement errors the differences in the values of r_{3954} for a sunspot and its surroundings were not revealed.

The operating plates also contain the spectra of the disk centre and portions of the undisturbed disk at the same angular distance ϑ as the studied sunspots. Except the spectrograms, mentioned above, for some sunspots the photographs of the solar limb were obtained to estimate the effect of light scattering in the atmosphere and the optics of the telescope. The limb was photographed after the sunspot exposure. The slit was set in the polar region, parallel to the disk radius.

Spectrograms were recorded both along and across the dispersion direction. Microphotometer readings of the former type were used for drawing the emission reversal profiles. Scanning was carried out in 15—20 points of the sunspot and the surrounding plages. Records across the direction of dispersion were made in the region of the local continuum 3954.2 Å, in the centres of the H- and K-lines and in the intensity minimum of line H (H_1).

Considerable attention was paid to the quality control of the characteristic curves. This is described in more detail in a paper by one of the authors (Efendeva, 1973). It describes the way in which the sensitivity changes of a photometric system within the wavelength interval between lines H and K were accounted for. This method was suggested for reducing the observed ratios of the central residual intensities $r_{(K_3)}/r_{(H_3)}$, however, it does not permit $r_{(K)}$ and $r_{(H)}$ to be determined. Therefore, in the present paper we have measured the relative sensitivity of the photometric system in another way. The absolute intensities of the local continuum "windows" in the spectrum region of interest were applied to Houtgast's data (1970). These windows are insufficient to cover the whole wavelength interval on the plates totally. In addition, measurements by White and Suemoto (1968), contained in Table 2, were taken. On some photographs of the step wedge and the special spectrograms of the disk centre, intensities of 20—24 points, equally spaced within the wavelength, were measured; their "residual intensities" (with respect to 3954.2 Å) were compared with the corresponding values of Hougast's or White's and Suemoto's data, and the correction factors D_λ were determined, by which all residual intensities should be multiplied to reduce them to one common system. After averaging over the spectrograms, mentioned above, the D_λ-values were plotted as a function of λ. The correction factors for the cores of the H- and K-lines were determined by interpolating between the measured values.

Figure 1 shows an example for one of the plates. Here the correction curve has a typical form for many plates: the sensitivity of the system is almost unchanged in the region between H and K; near the plate edges, independently of the wavelength, it increases (or decreases) sharply.

The D_λ-correction factors enable us to express all intensities in continuum units at 4000 Å. For an umbra one should take into account the small differences in the continuum spectrum, following

from its model. According to the model computations by Henoux (1969) $I_{cK}/I_{c4000}=0.967$ and $I_{cK}/I_{c4000}=0.984$. For the penumbra (model computations by Kjeldseth Moe and Maltby, 1969) and the quiet photosphere (HSRA model, Gingerich et al., 1971) the slope of the continuum

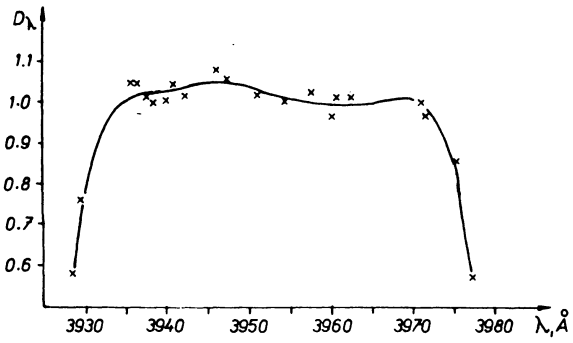

Fig. 1. The correction factor, taking into account the change in the sensitivity of a photometric system in the spectrum region under consideration.

between K, H and 4000 Å is practically zero.

The values $d_2=D_K/D_H$ are the factors for correcting the observed residual intensity ratios $r_{(K_3)}/r_{(H_3)}$. In Figure 2 the values are compared with the d_1 correction factors found in the quoted paper of Efendeva by comparison with the

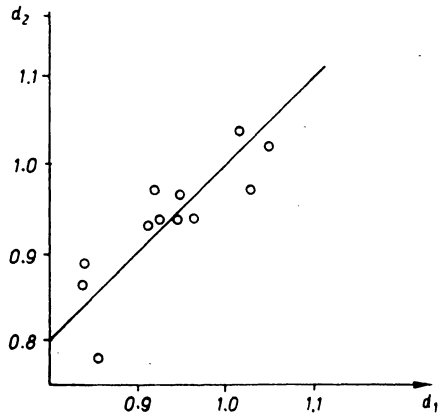

Fig. 2. Comparison between correction factors of the value $r_{(K_3)}/r_{(H_3)}$, defined in two different ways (see text).

photo-electric measurements of $r_{(K_3)}/r_{(H_3)}$ in the quiet atmosphere. Some differences between d_1 and d_2, except measurement errors, may be due to real observational conditions. All sunspots under consideration are located near the disk centre. Therefore, the reference spectrograms of the disk centre may be free of weak facular fields, but incompletely. Hence, $r_{(K_3)}/r_{(H_3)}$, measured at the disk centre, are not necessarily totally adequate for those in the quiet region.

Observational data were obtained over a period of three years. In early 1971 the old grating was replaced with a new one which had small light scattering. Its total intensity, together with the "ghosts", is 0.3%. The grating, used until 1971, was of a worse quality. "Ghosts" and the scattered light amounted to 4.0%. All the measured intensities are corrected in accordance with the figures given above. The profiles of the H- and K-lines in the disk centre, averaged over all plates, indicate the reliability of the measurements (Fig. 3). The r.m.s. difference of the mean value is 0.6% of the continuum intensity, or 10% of the measured value. However, the profiles of the H- and K-lines coincide, on the average, with the photo-electric data of other authors with an accuracy which could not be expected to be better in the photographic measurements.

Photometric trackings at 3954.2 Å and in H_1 are used for defining the umbra boundaries and the dimensions of the umbra and penumbra. More detailed information about it can be found in the authors' paper (1971).

In conclusion of this section we present Table 1 which includes the data on the observed sunspots, namely, the number of the plate, the date of observation, the number of the group according to the "Solar Data" bulletin, the sunspot area in millionths of the hemisphere, the mean sunspot diameter, measured on the image with a scale of $d_\odot=55$ cm, and the heliocentric sunspot location, sin ϑ.

Estimating the Amount of Stray Light

In determining the residual intensities of the lines in the sunspot spectrum, the main difficulty is the elimination of the scattered light of the atmosphere and the instrument. In particular, the central residual intensities of the H- and K-lines in the umbra are subjected to great distortions, because the intensities of the bright peaks are hardly affected by the scattered light, and the error of the continuum intensity measurements at 4000 Å reaches 100% of the value to be found even under favourable conditions. As a result, the values $\bar{r}^*=\bar{I}^*/\bar{I}^*$, measured in the cores of the H- and K-lines, may be 2—3 times less than the true

Table 1

Plate number	Data of observ.	Group number	S_p	d''	sin θ
489	17. 07. 1968	275	294	12	0.19
566	24. 10. 1969	376	230	17.5	0.05
573	26. 10. 1969	382	1285	24.5	0.15
576	26. 10. 1969	382	1285	24.5	0.15
581	27. 10. 1969	382	1085	19.5	0.33
599	18. 01. 1970	22	283	15	0.18
612	22. 01. 1970	28	196	17,5	0.21
624	28. 01. 1970	40	136	16	0.07
661	5. 07. 1970	315	1326	18	0.35
773	18. 09. 1971	323	158	11	0.24
775	19. 09. 1971	323	102	12	0.04
787	1. 10. 1971	333	432	20	0.28

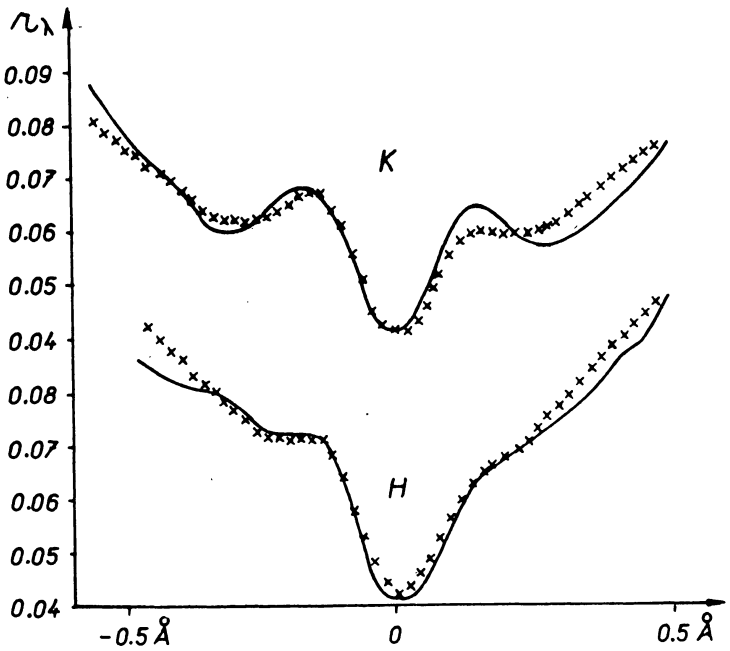

Fig. 3. Comparison of the measured line profiles, H and K, in the undisturbed chromosphere (solid curves) with results of the photo-electric measurements by White and Suemoto (crosses).

$r_\lambda = I_\lambda / I_c$. This was taken into account hardly by anyone who investigated the behaviour of the H- and K-lines in the sunspots. Only the observations by Paciorek (1965), calibrated by means of the continuum intensities in the disk centre, are free, to a considerable extent, of the scattered light effects.

The amount of scattered light is usually defined by the distribution of brightness near the limb and in the aureola. A detailed correction technique has been developed. It is described, in particular, by Stepanov (1957), Zwaan (1965), and Staveland (1970).

The investigated sunspots were located in the vicinity of the solar disk centre and some of them were very large. For such sunspots the main contribution is assumed to be made by the proper scattered light ("scattering" or "aureola"). Some authors (Staveland, 1970; Mattig, 1971) have noted that a considerable fraction of the scattered light enters from the penumbra due to a blurred image ("blurring").

For some plates (573, 576, 599, 624, and 661) additional photographs of the limb and the aureola were available. For these sunspots one could define an umbra contrast in the continuum,

$\varphi^* = I_c^*/I_c^\odot$, by usual methods, the relative scattered light caused by the aureola, $i_c/\tilde{I}_c^\odot$, the blurring parameter b, and the fraction of proper scattered light ε. The true contrast is related to the observed, $\tilde{\varphi}^* = \tilde{I}_c^*/\tilde{I}_c^\odot$, by Mattig's relationship (1971):

$$\varphi^* = \frac{\tilde{\varphi}^* - \frac{i_c}{\tilde{I}_c^\odot} - (1-\varepsilon)\left[\frac{I_c^+}{\tilde{I}_c^\odot}\Sigma_2 + \frac{I_c^\odot}{\tilde{I}_c^\odot}\Sigma_3\right]}{\left[1 - \frac{i_c}{\tilde{I}_c^\odot}\right]\Sigma_1} \qquad (1)$$

where I_c^* is the true continuum intensity in the umbra centre, $I_c^\odot$ the same in the surrounding undisturbed photosphere, $\tilde{I}_c^\odot$ the continuum intensity measured in the surrounding undisturbed photosphere, $\tilde{I}_c^*$ the continuum intensity measured in the umbra centre, and I_c^+ the continuum intensity in the middle of the penumbra (an assumption is made that it is not distorted by scattered light),

$$\Sigma_1 = \sum_1^n m_i(1 - \exp[-r^{*2}/b_i^2]),$$

$$\Sigma_2 = \sum_1^n m_i[\exp(-r^{*2}/b_i^2) - \exp(-r^{+2}/b_i^2)], \qquad (2)$$

$$\Sigma_3 = \sum_1^n m_i \exp(-r^{+2}/b_i^2).$$

Here r^* and r^+ are the umbra and penumbra radii, respectively. It is suggested that the blurring function may be represented as a sum of the Gaussians $\Psi_b = \sum_1^n \frac{m_i}{\pi b_i^2}\exp(-r^2/b_i^2)$, $\sum_1^n m_i = 1$; b_i are the blurring parameters.

To estimate the scattered light due to the aureola, we have sought a scattering function $\psi_s(r)$ in the form proposed by Stepanov (1957a, b):

$$\psi_s(r) = a_1 + a_2 \exp(-r/s^2), \qquad (3)$$

where s is the halfwidth of the scattering function. Measurements of the intensity in the aureola were used and the relative scattered light at the point where the sunspot was located, $i_c/\tilde{I}_c^\odot$, was defined with the help of additional functions $F(s, \varrho)$ and $F(s, \varrho)/F(s, 0)$, computed by Stepanov. Here ϱ is the distance from the disk centre, expressed in units of the solar radii. Stepanov used the sum of two exponents in (3), and we have confined ourselves to one exponent.

After defining the amount of scattered light due to the aureola, we have eliminated the latter when determining the brightness change in the direct vicinity of the limb and the estimated parameters b_i. The limb profile is satisfactorily described by a sum of two Gaussians with $b_1 = 2''.5 - 4''.5$ and $b_2 = 20'' - 30''$.

In order to determine parameter ε one may use Table 2,4 by Zwaan (1965). This value is obtained by means of the measurements of a relative aureole at the distance 1′ from the solar limb:

$$\eta(17') = \frac{\tilde{I}_c(17')}{\tilde{I}_c^\odot(0)}. \qquad (4)$$

Table 2 gives the observed contrasts for all sunspots and the corrected contrasts for five sunspots. The latter values have one common deficiency, typical for all methods which use non-simultaneous observations of the investigated object and of the brightness distribution near the limb: the visual conditions may change during the period between photographing the sunspots and the additional plates.

There are some methods for evaluating stray light, based on specific features of the operating spectrograms. Such methods were developed by

Table 2

Plate number	Quality	$\tilde{\varphi}^*$	φ^*	$\varphi\ddagger$	$\tilde{\varphi}^* - \varphi\ddagger$	$\frac{I_{4000A}^\odot\,\theta}{I_{4000A}^\odot(0)}$
566	4.5	0.133		0.050	0.083	0.999
573	3.9	0.147	0.091	0.050	0.097	0.991
576	3.0	0.114	0.048	0.056	0.058	0.991
581	3.9	0.099		0.059	0.040	0.947
599	3.2	0.182	0.095	0.071	0.111	0.987
612	3.6	0.182		0.038	0.144	0.982
624	3.4	0.169	0.053	0.050	0.119	0.998
661	5.0	0.50	0.034	0.030	0.020	0.928
773	4.0	0.118		0.081	0.037	0.977
775	2.5	0.202		0.037	0.165	0.999
787	4.8	0.052		0.032	0.020	0.969

Howard (1958) and Zwaan (1965). It seems that one may get the necessary information of this kind from the spectrograms of sunspots in the region of the H- and K-lines. The authors' paper (1973) Continuous absorption coefficients were taken from the data by Bode (1965). The measured values W_k^*, W_k^+ and $W_k^\odot$ were averaged over all available spectrograms of the umbra centre, the penumbra centre and the disk centre.

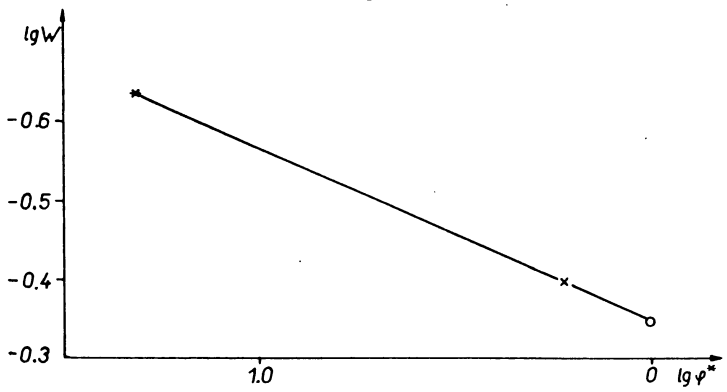

Fig. 4. Dependence of the emission width on the contrast (* — umbra, + — penumbra, ⊙ — photosphere).

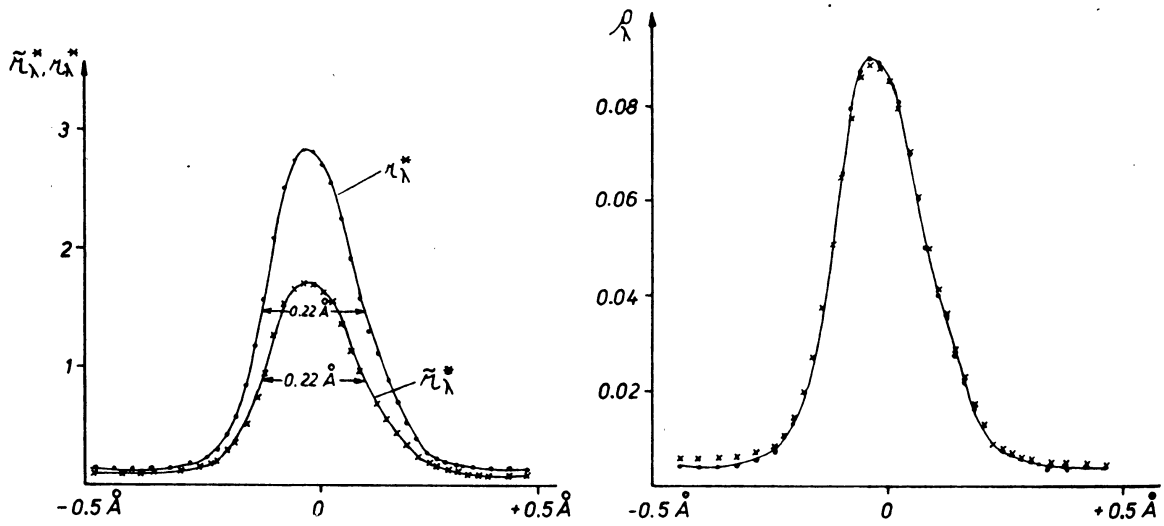

Fig. 5. Measured (crosses) and corrected (points) profiles of line K ("typical" profile, plate 787). a — calibration against the continuum in the spectrum of the umbra; b — calibration against the continuum in the spectrum of the disk centre.

shows that the width of the emission cores of the K- (or H-) line, W_k, depends on the "luminosity" of the solar formation under consideration. It was also found that W_k depends linearly on the contrasts $\varphi = I_c/I_c^\odot$, computed for a continuum at 4000 Å. Figure 4 shows the mean values of W_k in the umbra (*), the penumbra ($^+$) and the photosphere ($^\odot$), plotted against φ^*, φ^+ and 1. The contrast were computed for the umbra model of Henoux (1969) and for the penumbra model of Kjeldseth Moe and Maltby (1969), with respect to the photospheric model of Gingerich et al. (1971).

The measured values W_k^* are practically independent of the stray light (Fig. 5a). The accidental error in the width measurements is not more than 3%. Nevertheless, W_k^* of the different sunspots considerably deviate from the mean value given in Figure 4. We assume, first, that the deviations are due to the peculiarities of the individual sunspots, and secondly, that the individual sunspots are subject to the relationship $W_k(\varphi)$, given in Figure 4. If this so, then using Figure 4, we can find the true contrast. We denote it by φ_k^* to distinguish it from φ^*, defined after the usual elimination of the

scattered light. The determined values φ^*_w are given in Table 2. Comparing φ^* and φ^*_w of the sunspots for which the scattered light data are available, we can see that the agreement between them is satisfactory, especially if one takes into account the approximate character of the definition of φ^* when the photographs of the sunspot and the limb were taken at different moments.

Unlike φ^*, we know φ^*_w for all sunspots. It is interesting to note that the mean difference $(\tilde{\varphi}^* - \tilde{\varphi}^*_w)$ for 6 sunspots with visual estimates of the image quality $\leqq 3.5$ is twice the corresponding one >3.5 (Tab. 2). This may be considered as one more fact in favour of our estimate of the true contrast by means of the values of W^*_λ being based on reasonable assumptions.

To reduce the measured profiles, one should know not only the quantity of the stray light, but its source, too. For large sunspots of plates 581, 661, and 787, which were observed under good sky conditions, the main source of stray light is the aureola. This is supported by the direct measurements of scattered light for plate 661. In cases like this, the corrected residual intensity r^*_λ in the umbra centre is associated with the observed value $\tilde{r}^*_\lambda$ by the relationship:

$$r^*_\lambda = \frac{\tilde{\varphi}^* r^*_\lambda - r^\odot_\lambda \frac{i_c}{I^\odot_c}}{\tilde{\varphi}^* - \frac{i_c}{I^\odot_c}} \qquad (5)$$

$r^\odot_\lambda$ is the residual intensity of the line in the surrounding photosphere. For the large sunspots of plates 573 and 576, taken at a worse image quality, the contribution is made by blurring from the penumbra, too. For such sunspots

$$r^*_\lambda = \frac{\tilde{\varphi}^* \tilde{r}^*_\lambda - r^\odot_\lambda \frac{i_c}{\tilde{I}^\odot_c} - (1-\varepsilon)\frac{I^\odot_c}{\tilde{I}^\odot_c}\left(r_\lambda + \frac{I^+_c}{\tilde{I}^\odot_c}\Sigma_2 + r^\odot_\lambda \Sigma_3\right)}{\tilde{\varphi}^* - \frac{i_c}{\tilde{I}^\odot_c} - (1-\varepsilon)\frac{I^\odot_c}{\tilde{I}^\odot_c}\left(\frac{I^+_c}{\tilde{I}^\odot_c}\Sigma_2 + \Sigma_3\right)} \qquad (6)$$

Here r^+_λ is the residual intensity of the line the middle of the penumbra. In both Eqs (5) and (6) it is assumed that the line profiles in the aureola do not differ from those in the region surrounding the sunspot. Equation (6) should also be used for small sunspots under any visual conditions.

The values of r^*_λ, i.e. the line intensities, expressed in terms of the continuum intensity of the umbra, are needed to define the source functions in absolute units. However, for this purpose one can also use the line intensities, expressed in any known units, in particular, in terms of the continuum intensity of the disk centre. Denote them by ϱ^*_λ, i.e. $\varrho^*_\lambda = I^*_\lambda / I^\odot_{c(0)}$. The profiles in the paper by Paciorek (1965) are represented in these intensities. If one considers the central portions of the emission peaks, preference should be given rather to $\tilde{\varphi}^*_\lambda$ than $\tilde{r}^*_\lambda$; because $\tilde{\varrho}^*_\lambda$ are practically undistorted by the scattered light. Only in the H_1- and K_1-regions $\tilde{r}^*_\lambda$ and $\tilde{\varrho}^*_\lambda$ depend approximately equally on the scattered light (Fig. 5).

The differences $(\tilde{\varphi}^* - \varphi^*_w)$ and the visual estimates of the image quality, given in Table 2, may serve as a measure of the spectrogram quality. On plates 581, 661, 787, and 773 the difference $(\tilde{\varphi}^* - \varphi^*_w)$ is comparatively small (<0.05). We consider these plates as the best and most meaningful. Plates 566, 573, and 576 are plates of the second sort; for them $(\tilde{\varphi}^* - \varphi^*_w) \approx 0.1$.

Plates 573, 576 and the two spectrograms of plate 661 were treated with the help of the measured scattered light parameter. Plates 566, 581, and 787 were treated with the help of the values of φ^*_w on the assumption that the stray light source is the aureola. For high quality plate 773 the reduction in respect of the scattered light was performed in terms of φ^*_w too. This sunspot is small, therefore, a considerable role may be played by blurring. Computations were performed on three assumptions: all the stray light is due to the aureola; all the stray light is due to blurring from the penumbra; contributions of both effects are equal. The differences between the corrected profiles in the three alternatives did not appear to be large and the third alternative was finally adopted.

The other plates with $(\tilde{\varphi}^* - \varphi^*_w) > 0.1$ were considered as being of the third sort. Complete profiles of the H- and K-lines were not drawn. Only central residual intensities were defined. In the cases when the stray light was eliminated on the basis of the φ^*_w-values, it was assumed that, independent of the sunspot dimensions, blurring plays the same role as the scattering. Plates of the 3rd sort are suitable for determining the parameters which were distorted by the stray light but little: these are W_K, φ^*_K, φ^*_H and the asymmetry of the profiles.

Profiles of the Ca II H- and K-lines in the Umbra

For each sunspot three scans near the umbra centre were examined and profiles of the H- and K-lines were averaged over these scans. In some cases the most typical profiles of H and K for the umbra, i.e. those with the greatest residual intensity and the smallest width, were located not just in the umbra centre, but somewhat aside of it (Fig. 6). Therefore, apart from the mean profiles we also considered the most typical one for each sunspot.

The results of the measurements and the reduction surely enough confirm the considerable variability of the emission cores of H and K, both from one sunspot to the other and inside the umbra of one sunspot. The tops of the emission peaks are completely different. After eliminating the stray light, the H- and K-profiles in the individual sunspots differ less than before the reduction, but considerable discrepancies still remain. The most sharply distinguished is the smallest sunspot of the

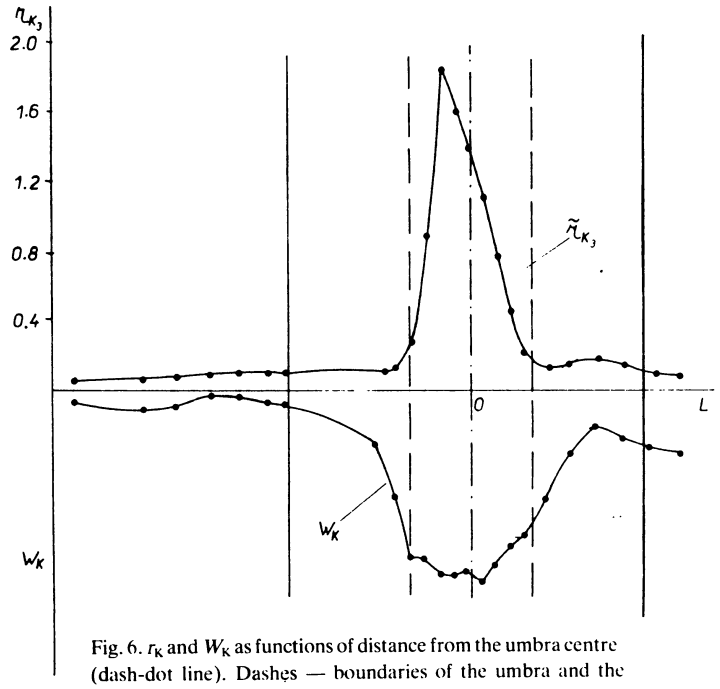

Fig. 6. r_K and W_K as functions of distance from the umbra centre (dash-dot line). Dashes — boundaries of the umbra and the penumbra; solid lines — sunspot boundaries (plate 787).

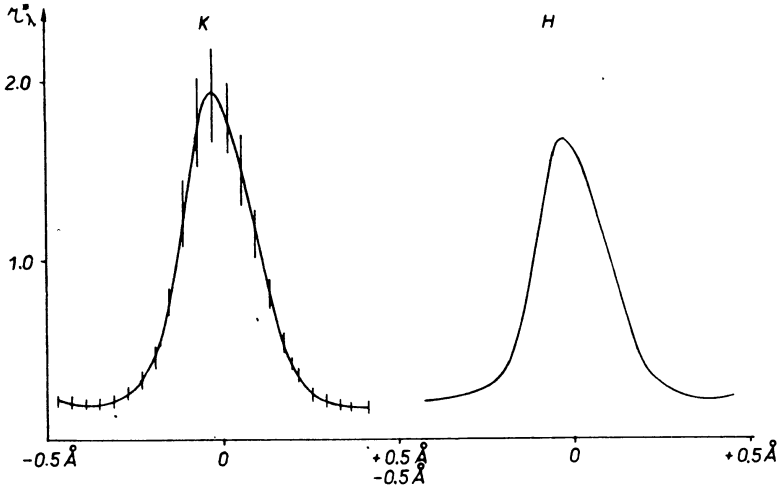

Fig. 7. H- and K-profiles averaged over 6 spectrograms in the "mean" scans of the large sunspot umbra.

Table 3. "Mean" profiles r_λ^*

Δλ,Å	K-line					H-line				
	581	661.1	661.2	787	SR.	581	661.1	661.2	787	SR.
1	2	3	4	5	6	7	8	9	10	11
−0.50		0.24	0.24			0.16				
0.48		0.24	0.24	0.13	0.20	0.15	0.36	0.26	0.13	0.22
0.46	0.17	0.24	0.24	0.13	0.19	0.16	0.35	0.26	0.12	0.22
0.44	0.18	0.24	0.23	0.13	0.20	0.16	0.34	0.26	0.12	0.22
0.42	0.19	0.24	0.23	0.13	0.20	0.18	0.33	0.26	0.13	0.22
−0.40	0.20	0.23	0.23	0.13	0.20	0.20	0.32	0.26	0.13	0.23
0.38	0.21	0.22	0.22	0.13	0.20	0.21	0.32	0.26	0.13	0.23
0.36	0.22	0.22	0.22	0.14	0.20	0.23	0.33	0.26	0.13	0.24
0.34	0.24	0.23	0.23	0.14	0.20	0.24	0.34	0.27	0.14	0.25
0.32	0.25	0.23	0.24	0.14	0.22	0.26	0.35	0.27	0.14	0.26
−0.30	0.28	0.25	0.25	0.15	0.23	0.28	0.37	0.27	0.15	0.27
0.28	0.32	0.28	0.28	0.16	0.26	0.32	0.38	0.27	0.16	0.29
0.26	0.37	0.31	0.28	0.19	0.29	0.36	0.43	0.28	0.20	0.32
0.24	0.42	0.35	0.30	0.24	0.33	0.42	0.47	0.30	0.23	0.35
0.22	0.48	0.41	0.34	0.34	0.39	0.49	0.53	0.31	0.29	0.40
−0.20	0.57	0.53	0.40	0.48	0.50	0.57	0.64	0.35	0.38	0.49
0.18	0.67	0.74	0.48	0.66	0.64	0.66	0.69	0.42	0.53	0.57
0.16	0.78	0.82	0.62	0.86	0.77	0.76	1.09	0.44	0.67	0.74
0.14	0.94	1.29	0.74	1.03	1.00	0.91	1.42	0.52	0.90	0.94
0.12	1.14	1.64	0.91	1.43	1.28	1.11	1.71	0.73	1.21	1.19
−0.10	1.35	1.90	1.19	1.74	1.54	1.31	1.92	0.97	1.43	1.41
0.08	1.53	2.25	1.58	1.98	1.84	1.48	2.02	1.22	1.65	1.59
0.06	1.67	2.40	1.79	2.12	2.00	1.60	2.04	1.68	1.72	1.76
0.04	1.74	2.36	1.99	2.08	2.04	1.64	2.00	1.72	1.70	1.77
−0.02	1.74	2.19	2.12	1.99	2.01	1.62	1.87	1.80	1.60	1.72
0.00	1.67	2.01	2.18	1.83	1.92	1.54	1.70	1.81	1.50	1.63
+0.02	1.53	1.84	2.10	1.67	1.78	1.41	1.51	1.77	1.34	1.51
0.04	1.37	1.61	1.96	1.46	1.60	1.26	1.33	1.67	1.16	1.35
0.06	1.19	1.35	1.72	1.26	1.38	1.10	1.16	1.56	1.00	1.21
0.08	1.03	1.17	1.46	1.12	1.19	0.94	1.01	1.54	0.86	1.09
0.10	0.87	1.02	1.18	1.02	1.02	0.78	0.90	1.19	0.71	0.90
0.12	0.74	0.91	0.89	0.85	0.85	0.66	0.78	1.00	0.61	0.76
0.14	0.65	0.79	0.71	0.66	0.70	0.58	0.67	0.79	0.49	0.63
0.16	0.55	0.64	0.57	0.50	0.56	0.52	0.58	0.64	0.40	0.54
0.18	0.47	0.50	0.42	0.40	0.45	0.45	0.49	0.50	0.32	0.44
0.20	0.42	0.40	0.49	0.31	0.40	0.40	0.42	0.39	0.25	0.36
0.22	0.36	0.32	0.29	0.22	0.30	0.35	0.38	0.37	0.20	0.32
0.24	0.31	0.29	0.27	0.18	0.26	0.32	0.35	0.31	0.16	0.28
0.26	0.27	0.25	0.25	0.16	0.23	0.29	0.34	0.27	0.17	0.27
0.28	0.24	0.23	0.24	0.14	0.21	0.26	0.33	0.26	0.17	0.26
0.30	0.22	0.21	0.23	0.13	0.20	0.24	0.33	0.26	0.18	0.25
0.32	0.20	0.20	0.22	0.13	0.19	0.21	0.32	0.25	0.18	0.24
0.34	0.19	0.20	0.22	0.13	0.18	0.20	0.31	0.25	0.18	0.24
0.36	0.17	0.21	0.22	0.13	0.18	0.19	0.31	0.25	0.18	0.23
0.38	0.16		0.22	0.13	0.17	0.18	0.30	0.25	0.16	0.22
0.40	0.15		0.22	0.13	0.17	0.17	0.30	0.26	0.14	0.22

Table 4. "Typical" profiles r_λ^*

$\Delta\lambda$,Å	K-line					H-line				
	581	661.1	661.2	787	SR	581	661.1	661.2	787	SR
1	2	3	4	5	6	7	8	9	10	11
−0.48		0.25		0.13	0.19	0.15	0.39		0.14	0.23
0.46	0.17	0.24	0.24	0.13	0.20	0.16	0.39		0.14	0.23
0.44	0.18	0.24	0.24	0.13	0.20	0.18	0.40	0.24	0.14	0.24
0.42	0.18	0.23	0.26	0.13	0.20	0.20	0.40	0.26	0.14	0.25
−0.40	0.20	0.23	0.26	0.12	0.20	0.22	0.40	0.28	0.15	0.26
0.38	0.20	0.23	0.24	0.12	0.20	0.24	0.36	0.28	0.16	0.26
0.36	0.22	0.24	0.22	0.12	0.20	0.26	0.32	0.25	0.16	0.25
0.34	0.26	0.24	0.24	0.13	0.22	0.29	0.31	0.24	0.16	0.25
0.32	0.29	0.25	0.25	0.14	0.23	0.32	0.32	0.25	0.16	0.26
−0.30	0.34	0.25	0.25	0.16	0.25	0.35	0.33	0.28	0.16	0.28
0.28	0.43	0.26	0.28	0.18	0.29	0.39	0.35	0.32	0.16	0.31
0.26	0.45	0.27	0.31	0.20	0.31	0.44	0.36	0.32	0.18	0.33
0.24	0.52	0.30	0.35	0.22	0.35	0.50	0.38	0.32	0.23	0.36
0.22	0.58	0.32	0.36	0.29	0.39	0.56	0.39	0.34	0.28	0.39
−0.20	0.66	0.38	0.40	0.42	0.46	0.63	0.42	0.34	0.36	0.44
0.18	0.75	0.47	0.47	0.58	0.57	0.71	0.48	0.39	0.46	0.51
0.16	0.87	0.62	0.57	0.84	0.73	0.84	0.55	0.49	0.62	0.62
0.14	1.03	0.82	0.71	1.18	0.94	1.02	0.63	0.55	0.88	0.77
0.12	1.23	1.20	0.87	1.58	1.22	1.24	0.91	0.72	1.16	1.01
−0.10	1.50	1.57	1.16	2.09	1.58	1.47	1.23	0.95	1.49	1.29
0.08	1.68	1.96	1.52	2.51	1.92	1.69	1.54	1.34	1.90	1.62
0.06	1.86	2.26	1.94	2.76	2.21	1.85	1.85	1.60	2.26	1.89
0.04	2.02	2.42	2.26	2.85	2.39	1.90	2.04	1.94	2.35	2.06
0.02	2.00	2.49	2.38	2.82	2.42	1.86	2.09	2.06	2.34	2.09
0.00	1.94	2.42	2.33	2.70	2.35	1.76	2.02	1.91	2.30	2.00
+0.02	1.79	2.16	2.30	2.55	2.20	1.60	1.97	1.90	2.17	1.91
0.04	1.55	1.68	2.18	2.25	1.92	1.38	1.80	1.77	1.99	1.73
0.06	1.30	1.54	1.98	1.91	1.69	1.16	1.60	1.62	1.72	1.53
0.08	1.07	1.32	1.80	1.58	1.45	1.00	1.40	1.46	1.36	1.30
0.10	0.91	1.11	1.52	1.30	1.21	0.84	1.18	1.26	1.09	1.16
0.12	0.78	1.02	1.25	1.14	1.05	0.70	1.07	0.98	0.95	0.92
0.14	0.68	0.96	0.98	0.90	0.93	0.62	0.98	0.84	0.82	0.82
0.16	0.58	0.83	0.67	0.70	0.69	0.54	0.80	0.58	0.69	0.65
0.18	0.50	0.66	0.53	0.53	0.56	0.48	0.69	0.46	0.54	0.54
0.20	0.45	0.53	0.41	0.40	0.44	0.42	0.58	0.40	0.41	0.45
0.22	0.40	0.38	0.29	0.27	0.34	0.36	0.50	0.33	0.34	0.38
0.24	0.35	0.31	0.25	0.24	0.29	0.32	0.44	0.26	0.29	0.33
0.26	0.30	0.27	0.30	0.21	0.27	0.29	0.37	0.23	0.25	0.29
0.28	0.28	0.24	0.28	0.18	0.24	0.27	0.34	0.23	0.21	0.26
0.30	0.25	0.24	0.27	0.16	0.23	0.26	0.32	0.26	0.18	0.25
0.32	0.24	0.21	0.25	0.15	0.21	0.24	0.31	0.27	0.15	0.24
0.34	0.22	0.20	0.25	0.14	0.20	0.24	0.31	0.28	0.13	0.24
0.26	0.19	0.19	0.25	0.14	0.19	0.23	0.31	0.27	0.13	0.23
0.38	0.19	0.19	0.25	0.13	0.19	0.21	0.31	0.27	0.14	0.23
0.40	0.17		0.25	0.13	0.18	0.20	0.30	0.25	0.15	0.23
0.42	0.14		0.25	0.12	0.17	0.19	0.30	0.25	0.16	0.22
0.44	0.14		0.25	0.12	0.17	0.20	0.30	0.26	0.17	0.23
0.46	0.14		0.25			0.20	0.30	0.31	0.18	0.25

Table 5

$\Delta\lambda$, Å	"Mean" profile r^*_λ		"Typical" profile	
	K-line	H-line	K-line	H-line
1	2	3	4	5
−0.48	0.111	0.116	0.120	0.131
0.46	0.110	0.113	0.119	0.126
0.44	0.110	0.118	0.119	0.128
0.42	0.108	0.124	0.117	0.136
−0.40	0.106	0.132	0.115	0.144
0.38	0.107	0.140	0.112	0.148
0.36	0.107	0.143	0.107	0.152
0.34	0.106	0.144	0.109	0.152
0.32	0.106	0.143	0.117	0.150
−0.30	0.111	0.137	0.128	0.151
0.28	0.120	0.138	0.138	0.153
0.26	0.131	0.146	0.154	0.158
0.24	0.148	0.155	0.171	0.166
0.22	0.173	0.169	0.191	0.183
−0.20	0.198	0.191	0.216	0.212
0.18	0.225	0.221	0.248	0.255
0.16	0.278	0.254	0.286	0.320
0.14	0.317	0.305	0.338	0.393
0.12	0.391	0.378	0.425	0.478
−0.10	0.476	0.450	0.538	0.555
0.08	0.558	0.511	0.635	0.608
0.06	0.625	0.545	0.692	0.637
0.04	0.652	0.560	0.740	0.643
0.02	0.652	0.560	0.740	0.642
0.00	0.627	0.547	0.720	0.622
+0.02	0.596	0.518	0.685	0.587
0.04	0.563	0.480	0.640	0.550
0.06	0.527	0.438	0.602	0.500
0.08	0.484	0.397	0.565	0.445
0.10	0.440	0.348	0.517	0.392
0.12	0.395	0.300	0.455	0.336
0.14	0.350	0.262	0.381	0.272
0.16	0.303	0.224	0.307	0.216
0.18	0.256	0.190	0.252	0.174
0.20	0.206	0.163	0.206	0.151
0.22	0.168	0.144	0.168	0.144
0.24	0.139	0.133	0.141	0.139
0.26	0.118	0.127	0.122	0.134
0.28	0.116	0.123	0.114	0.130
0.30	0.101	0.126	0.107	0.128
0.32	0.098	0.128	0.101	0.129
0.34	0.098	0.124	0.100	0.128
0.36	0.099	0.117	0.099	0.131
0.38	0.101	0.114	0.098	0.132
0.40	0.104	0.120	0.099	0.133
0.42	0.103	0.131	0.100	0.136
0.44	0.102	0.141	0.102	0.140
0.46	0.101	0.149	0.101	0.146

1st sort (plate 773). For this reason the averaging a small number of sunspots with similar characteristics. This information can be found in Tables 3, 4, 5 and in Figure 7.

Table 3 gives the residual intensities averaged over 3—4 scans in the umbra of large sunspots of the three best plates 581, 661, 787. In Table 4 the same values are given not for the mean profiles, but for the most typical ones. Table 5 shows analogous data for a small sunspot on plate 773.

Figure 7 gives H- and K-profiles averaged over all plates of the 1st and 2nd sort for sunspots with $d \geqq 17.5''$, i.e. measurements of plates 566, 573, 576, 581, 661 (two spectrograms), and 787 were taken into account. The dimensions of the vertical bars correspond to the dispersion of the individual values with respect to the mean. This dispersion is due to random measurement errors, uncertainties in determining the correction factors D_λ, a lack of accurate information on the parameters of the blurring and scattering functions, but mostly to the difference of the H- and K-lines in the sunspot spectra, mentioned above. One can see it best of all in the two spectrograms of plate 661. The spectrograms were obtained one after the other

Table 6

N	$\bar{r}^*_{(K_3)}$	$r^*_{(K_3)}$ K-line	$\varrho^*_{(K_3)}$	$r^*_{(H_3)}$	$r^*_{(H3)}$ H-line	$\varrho^*_{(H3)}$
			"Mean" profiles			
566	0.577	1.520	0.074	0.480	1.215	0.063
573	1.080	1.641	0.152	0.927	1.399	0.133
576	0.998	2.036	0.111	0.920	1.823	0.102
581	1.032	1.745	0.093	0.978	1.645	0.090
599	0.496	1.410	0.084	0.386	1.094	0.068
612	0.544	2.707	0.095	0.462	2.209	0.081
624	0.805	2,356	0.131	0.630	1.786	0.104
661.1	1.610	2.400	0.072	1.365	2.040	0.062
661.2	1.445	2.180	0.064	1.222	1.810	0.056
773	0.458	0.652	0.051	0.398	0.560	0.045
775	0.361	1.801	0.070	0.300	1.450	0.060
787	1.280	2.120	0.063	1.047	1.720	0.051
			"Typical" profiles			
566	0.656	1.757	0.084	0.530	1.376	0.069
573	1.230	1.887	0.173	1.040	1.588	0.149
576	1.050	2.124	0.116	0.930	1.858	0.104
581	1.192	2.025	0.108	1.126	1.002	1.104
599	0.603	1.855	0.106	0.483	1.433	0.085
612	0.607	3.066	0.105	0.527	2.579	0.093
624	0.805	2.356	0.131	0.630	1.786	0.104
661.1	1.675	2.490	0.075	1.387	2.090	0.063
661.2	1.590	2.380	0.072	1.395	2.065	0.064
773	0.515	0.740	0.058	0.435	0.643	0.052
775	0.386	1.952	0.075	0.327	1.613	0.065
787	1.712	2.850	0.083	1.425	2.350	0.071

with an interval of some seconds and are related to the neighbouring parts of the umbra of the same sunspot; conditions of photometry and reduction are identical, Meanwhile the differences in the profiles, particularly for the H-line, are striking. They are appreciable even on visual examination of the plate.

In all the tables and in Figure 7 the distances $\Delta\lambda$ are read from the catalogue wavelength values of the H- and K-lines (Moore et al., 1966).

Table 6 gives the observed and corrected maximum intensities at 4000 Å in the umbra spectrum ($\bar{r}^{\bullet}_{(K_3)}$, $r^{\bullet}_{(K_3)}$), as well as in the spectrum of the quiet solar disk centre ($\varrho^{*}_{(K_3)}$. The values of $\bar{\varrho}^{*}_{(K_3)}$ are not presented; they differ from the correct ones, but no more than by 5 %.

To reduce the number of tables, we do not give tables of the values of φ^{*}_{λ}. These data, however, are very useful, because they depend on the stray light parameters but little. With little computation one can proceed from r^{*}_{λ} of Tables 3, 4 and 5 to ϱ^{*}_{λ}; $\varrho^{*}_{\lambda} = r^{*}_{\lambda}\varphi^{*}(I^{\odot}_{4000(\theta)}/I^{\odot}_{4000(0)})^{\frac{1}{c}}$, where for the K-line $c = 0.967$, for the H-line $c = 0.984$. The values of φ^{*} or φ^{*}_{w} are given in Table 2. The last column contains the data of solar limb darkening near 4000 Å.

The Basic Properties of the Line Profiles of H and K in the Umbra

The basic properties of the H- and K-profiles have been described by many authors (Mustel and Tsap, 1960a, b; Bumba, 1960; Piacorek, 1965; Engvold, 1967; Linsky, 1970). We shall enumerate them once more, mostly emphasizing the quantitative relationships resulting from the photometric treatment of the observational material.

(a) The central depression of the emission reversals K_{232} and H_{232} in the umbra is expressed less distinctly than in the plages or in the penumbra. A detailed analysis was performed by Engvold (1967): he discovered depression almost in all sunspots. However, in our previous paper (1971) doubt was expressed as to this statement: the central depression is seen along the whole umbra only in sunspots located at distances from the disk centre exceeding about 45°. The absence of this depression in the central parts of the umbra, located near the disk centre, is supported by the photometric reduction carried out in the present paper.

(b) The emission core widths of K and H in the umbra are much smaller than in the plages. Detailed data on the width of the core K, W_K, are given in another paper (Teplitskaya and Efendeva, 1973).

(c) The largest difference of the H- and K-lines in the umbra from those in any other solar region is in the extremely high central residual intensities $r_{(K_3)}$ and $r_{(H_3)}$. The cases often occur when the latter are greater than 2 and are compared with the corresponding values in the flares. At the same time, the central residual intensities vary more than other characteristics from one sunspot to another and inside the umbra of one sunspot. This is the main thing that causes difficulties when the typical H- and K-profiles for sunspots are being drawn.

The enhanced chromospheric brightness above the sunspot is reflected even more clearly by the values of $\varrho^{\bullet}_{(K_3)}$ and $\varrho_{(H_3)}$. Provided $\varrho^{\bullet}_{(K_3)}/r^{\odot}_{(K_3)} = I^{\bullet}_{(K_3)}/I^{\odot}_{(K_3)}$, where $I_{(K_3)}$ is the intensity of the emission peak, the obtained umbra brightness is often several times larger than that of the quiet chromosphere ($r^{\odot}_{(K_3)} = 0.0413$). Note that in some scans Paciorek even obtained $\varrho^{+}_{(K_3)}$ (in her notations I_P) equal to 0.22. This value is probably too high as the transition from the continuum bear 3854 Å to that near 4000 Å is made according to the Utrecht Atlas.

In connection with the central residual intensities, it is interesting to consider the photometric trackings across the direction of dispersion in K_3 (or H_3). The values of $I_{(K_3)}$ vary rather randomly in the sunspot and its neighbourhood (plate 787, Fig. 8a). Only in three cases (plates 566, 581, 661, Fig. 8b) a semblance of a sunspot remains at the level of the K_3-formation. The sunspot is sometimes distinguished against a background of surrounding plages only at one side (Fig. 8c). On all records, however, the region inside the umbra is characterized, on the average, by a smaller intensity than in the plages; the minimum intensity being close to or higher than that of the most distant undisturbed regions. Thus, in the layers where H_3 and K_3 are formed, a sunspot is distinguished as an individual formation only against a background of enhanced brightness of the plages. As for the quiet chromosphere, it could be seen as a bright object, or could not be seen at all.

(d) The ratios of the central residual intensities $r_{(K_3)}/r_{(H_3)}$ are gradually increased from the sunspot periphery to the umbra centre (Efendeva, 1973). More accurately these ratios, according to the second section are as follows:

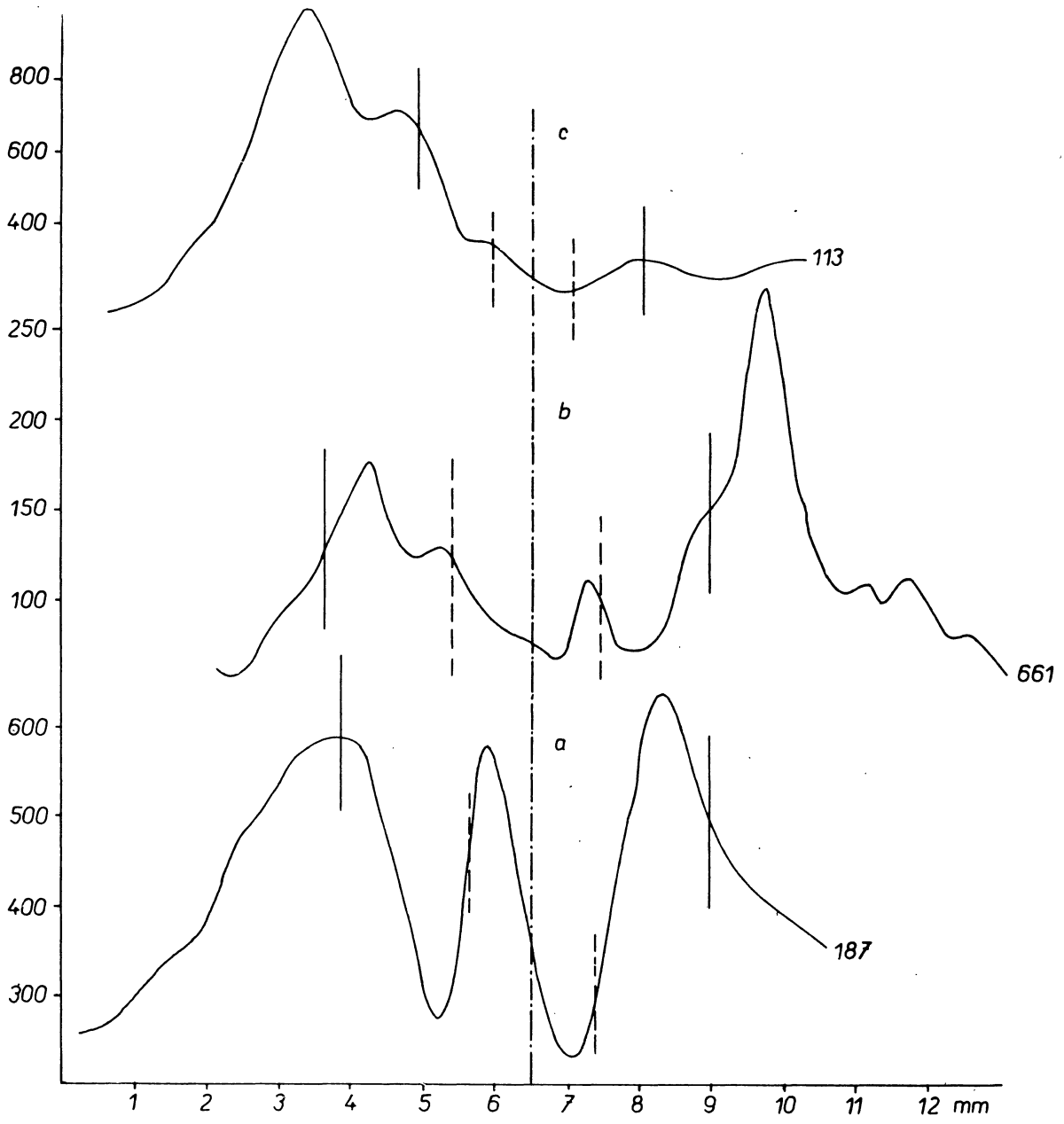

Fig. 8. Photometric tracings across the direction of dispersion in the centre of line K. The lines are the same as in Figure 6.

umbra	1.20 ± 0.06;
penumbra	1.03 ± 0.06;
bright ring	1.01 ± 0.06;
plages	1.06 ± 0.08;
quiet region	1.00 ± 0.04.

The values of $r_{(K3)}/r_{(H3)}$ for the plages and the quiet chromosphere are in good agreement with the recent results of Shine and Linsky (1972). For the umbra this ratio is much less than that measured for one sunspot near the disk centre. The increase of this ratio to the umbra centre is, however, undoubtful.

(e) The asymmetry of the H- and K-profiles, mentioned often by many authors, consists in that the violet side of the emission peaks has a steeper slope than the red one. Besides, the violet shift of the intensity maximum with respect to the catalogue position of the line centres of H and K is, on the average, 0.03 Å.

To evaluate the asymmetry quantitatively the

wavelengths of the emission peaks will be determined more accurately. The results will be published later on.

Profiles of the H- and K-lines in the Penumbra

In each spectrogram the regions close to the middle of the penumbra were sampled. The stray light correction was not applied. The H- and K-profiles, corresponding to the chosen regions, are used for constructing the mean profiles, shown in Figure 9. The differences between the individual profiles, involved in the mean, are rather essential. The intensities of the peaks, the depression of H_3 and K_3, as well as the character of the asymmetry are changed. The dotted lines in Figure 9 are the K-profiles on two plates, corresponding to the greatest deviations from the mean values.

Paciorek (1965) and Engvold (1967) have observed opposite asymmetry signs on each side of the sunspot centre. None of our spectrograms show this, apparently because of the different positions of the sunspots on the disk. Both the present authors have studied sunspots, the heliocentric distance of which was more than 45°.

As for the sunspots located in the central part of the disk, we are faced with the other distinctly displayed feature of the asymmetry. In 23 scans out of 25, related to the middle of the penumbra, the violet peak of the K-line was brighter than the red one and in 2 scans both peaks were equal. As for the H-line, the relationship between the H_2 peak intensities is quite different. Only in 12 scans was the violet peak brighter than the red; in the remaining cases the intensities were either equal (5 scans), or the red peak was brighter (8 scans). Even when the violet peak was brighter, $r_{(H_{2v})}/r_{(H_{2r})}$ was less than $r_{(K_{2v})}/r_{(K_{2r})}$. This inequality can be seen well on the mean profiles in Figure 9.

The H-line is also characterized by a smaller amplitude of the intensity variation and the K-line.

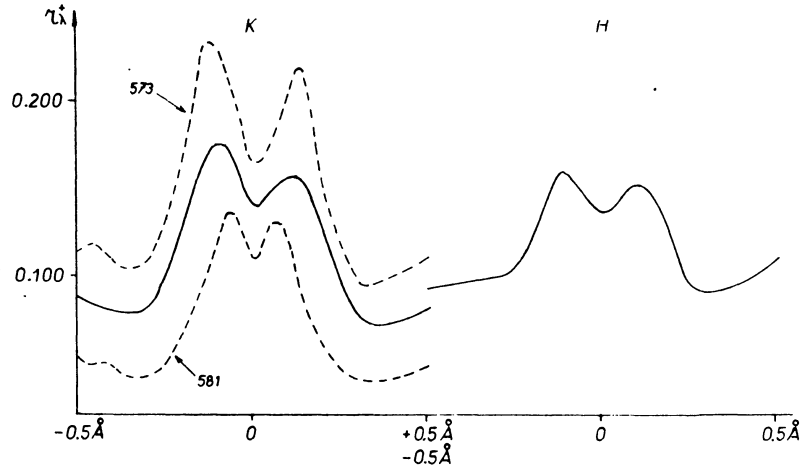

Fig. 9. H- and K-profiles averaged over all scans in the middle of the penumbra (solid curves). Profiles of line K on plates 573 and 581 (dashes).

Source Functions for the H- and K-line in the Umbra

It is desirable to use data presented in Tables 3, 4 and 5 for evaluating the physical conditions in the chromospheric layers of the sunspots. A similar study, founded on the low-chromospheric model and using observed data of the Ca II H- and K-profiles, was made by Linsky (1968) for a quiet region. The problem was treated by means of the line transfer equation and the statistical equilibrium equations. The problem is simplified a great deal, if the radiation field is known. In the present paper we confine ourselves to the analysis of the

source function. It can be found by means of the inversion of the intensity integral.

We only know a few papers in which the solution of the latter problem is performed at one point of the disk, i.e. the distribution of the source function with depth is found along measured line profiles. Worall and Wilson (1969) have used Na D-lines in the spectrum of the solar disk centre. The inversion of the integral

$$I_\lambda = \int_0^\infty S_\lambda(\tau)\, e^{-\tau_\lambda} \phi_\lambda \, d\tau \qquad (7)$$

giving a specific line intensity, is carried out. Here τ is the optical depth in the centre of the line under consideration, τ_λ the optical depth at the distance $\Delta\lambda = \lambda - \lambda_0$ from the line centre, ϕ_λ the normalized line absorption coefficient, and S_λ the source function. The continuous absorption processes are neglected.

In the complete frequency redistribution S_λ is replaced by the function S, independent of the frequency.

Equation (7) may be solved if one approximates the function required correctly. Worrall and Wilson (1969) represented $S(\tau)$ in the following form: $S(\tau) = \sum_{K=0}^{n} C_K L_K(\tau)$, where $L_K(\tau)$ are Laguerre polynomials of the k-th order. We have preferred the following approximation:

$$S(\tau) = \sum_{K=0}^{n} A_K (\lg \tau)^K. \qquad (8)$$

The substitution of (8) into the intensity integral (7) requires a Laplace transformation for lg x in an arbitrary degree. It can be shown that the application of this procedure yields

$$I_v = \sum_{K=0}^{n} B_K [\lg \phi(a, v)]^K, \qquad (9)$$

where $v = \Delta\lambda / \Delta\lambda_D$.

A matrix expressing the relation between the coefficients a_K and B_K, as well as the discussion of the stability of the solution, will be published elsewhere.

In order to determine the coefficients B_K of the observed line profile, one should know the damping parameter a and the Doppler width $\Delta\lambda_D$. Wilson and Worrall (1969) have assumed a purely Doppler profile and selected $\Delta\lambda_D$ in such a way that the source functions, found for two lines of the doublet, D_1 and D_2, were equal at the given depth. For the lines of Ca II the latter assumption is proved insufficiently. For instance, the source functions of the H- and K-lines are not equal at the same depths of the quiet chromosphere (Linsky, 1970). One can expect the inequalities of two source functions in the sunspot umbra to be still greater, because the ratio $r_{(K_3)}/r_{(H_3)}$ is considerably higher here than in the other regions. Hence, $\Delta\lambda_D$ should be found by a method which is independent of the solution of Eq. (7).

The well-known Goldberg-Unno technique for defining $\Delta\lambda_D$ suggests the following:

1. the source functions of two multiplet lines are equal at the common depth;
2. the source functions do not depend on the frequency;
3. the frequency dependence of the line absorption coefficient is the same at all depths;
4. the absorption coefficient profile is purely Doppler;
5. there are no convective motions in the atmosphere (De Jager and Neven, 1972).

Assumption (2) coincides with the above adopted assumption of the complete frequency redistribution. The dependence of the absorption coefficient on the depth may be partially accounted for by measuring $\Delta\lambda_D$ at different points of the profiles, as is usual. Assumption (4) is unnecessary. One may modify the Goldberg method to render it reliable for the Voigt profile, too (Troyan, 1971). More important are the first and fifth limitations. We have determined $\Delta\lambda_D$ in two alternatives.

1st alternative: the usual Goldberg-Unno technique, i.e. it is assumed that at each point in the atmosphere $S_K = S_H$.

2nd alternative: The difference between $r_{(K_3)}$ and $r_{(H_3)}$ is assumed to be due to a large gradient of the function $S(\tau)$ and partly to the inequality in the source functions of the two lines. To be more certain, we assumed $r_{(K_3)}/r_{(H_3)} = 1 + \alpha$ (α = const.). We then adopted $S_K/S_H = 1 + \frac{1}{2}\alpha$. To find $\Delta\lambda_D$ it is sufficient to replace all $r_{H\lambda}$ by $r_{H\lambda}(1 + \frac{1}{2}\alpha)$ and to apply to the profile of line H, reduced in this manner, together with the measured profile of line K, the standard Goldberg-Unno procedure.

In both alternatives only the violet parts of the emission peaks were used. The strong asymmetry of the peaks is probably associated with the large-scale motions in the radiating layer. However, the absence of the central depression in the H- and K-lines, when the sunspot is located near the disk centre and its appearance, when the sunspot is displaced to the limb (Teplitskaya and

Efendeva, 1971), may be the evidence for clouds sunk above the umbra. They cause the absorption in the red wings only. In this case the observed asymmetry does not prevent the use of the violet wings to define $\Delta\lambda_D$. To make sure, we did not consider the very peak tops either.

To estimate the damping parameter

$$a = \tfrac{1}{4}\pi^{-1}\Gamma\lambda^2 c^{-1}\Delta\lambda_D^{-1}, \qquad (10)$$

where Γ is the damping constant, we computed this value for the upper layers of the known sunspot umbra models. Already in the upper photosphere the contribution of all line broadening mechanisms is small compared with the radiation damping. Therefore, for the chromosphere one may adopt

$$\Gamma = \gamma_R = 1.43 \times 10^8 \text{ sec}^{-1}. \qquad (11)$$

Substituting (11) and $\Delta\lambda_D$, found for each alternative, into Eq. (10), we estimated $a \approx 0.001$, i.e. the same as in the quiet chromosphere.

Using the technique, described by Toryan (1971), we have checked that this value of the parameter a does not require the found values of $\Delta\lambda_D$ to be rendered more accurate.

The solution of Eq. (7) for one of the spectrograms ("typical" profiles on plate 661.1, Tab. 4). The line profiles were used upto a distance of $\Delta\lambda = -0.30$ Å. The Goldberg-Unno method yields $\Delta\lambda_D = 0.074$ Å, and its modification for $S_K/S_H \neq 1$ yields 0.047 Å. The iteration procedure ($K = 1, 2, \ldots, n$) converges rapidly; the weighted means of the successive approximations upto $n = 6$ were adopted as solutions.

Figure 10 shows the source functions S_K and S_H, depending on the optical depth τ_K, in the centre of line K. For comparison the function S_K is also presented in the quiet chromosphere; it was computed in the same manner from Linsky's data (1970) (photo-electric profiles of H and K). The horizontal straight lines correspond to the values of the Planck function for some temperatures.

Figure 10b shows a comparison of the change in the source function of line K for two values of $\Delta\lambda_D$.

The results should be considered as preliminary in so far as the computed ratios S_K/S_H do not correspond to the assumptions which were adopted for the two alternatives. For $\Delta\lambda_D = 0.074$ Å S_K/S_H should equal 1, on the average, in the considered layer. For $\Delta\lambda_D = 0.047$ Å one should expect $S_K/S_H = 1 + \frac{1}{2}\alpha = 1.09$. Instead, we have 0.85 and 1.04, respectively. To obtain the best agreement, it is necessary to take into account the variation of $\Delta\lambda_D$ with depth, which we intend to do in the future.

Inspite of the fact that the solutions, shown in Figure 10, cannot be considered complete, they illustrate the basic features of the source functions in the umbra well enough:

1. The gradient of the source function in the umbra is much greater than in the quiet region. In the centre of the lines the values of S_K^* and S_H^* are considerably larger than the values of $S_K^\odot$ and $S_H^\odot$. This accounts for the majority of the observed peculiarities in the form of the H- and K-profiles in the umbra spectra and the features of the Ca spectroheliograms above the sunspots.

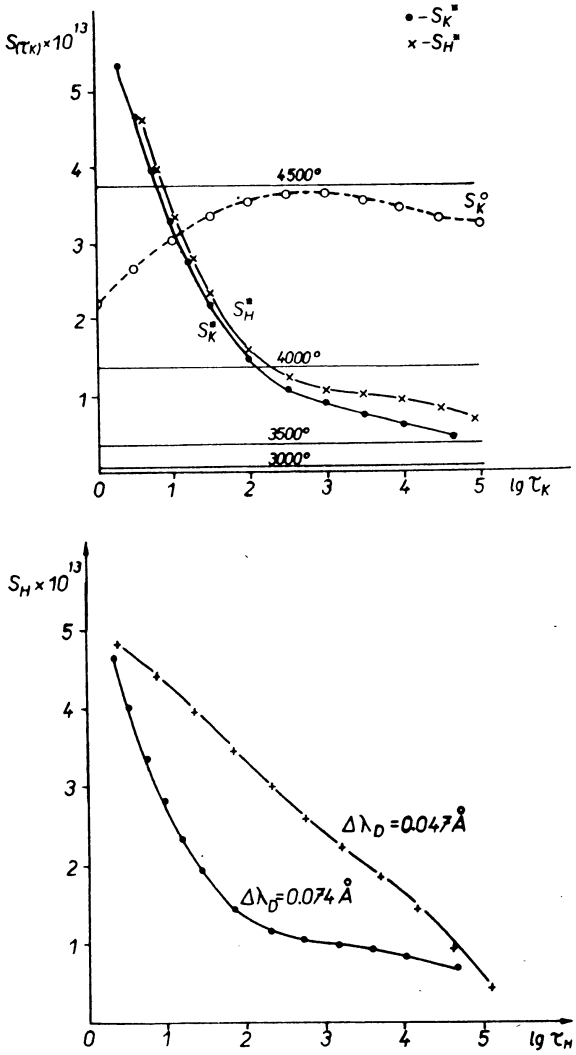

Fig. 10. a — Source functions of lines K, S_K, and H, S_H, in the umbra and undisturbed region as a function of the optical depth in the centre of line K. b — the source function of line K as a function of the optical depth in the centre of line K for two values of $\Delta\lambda_D$.

It is interesting that even of LTE conditions exist above the umbra and the temperature is not more than 5000 K, the umbra would seem brighter than the quiet chromosphere at the wavelengths of the central parts of the H- and K-lines.

2. We have observed the profiles of both lines upto $\Delta\lambda = 0.30$ Å. According to the Barbier-Eddington approximation, the optical depth $\tau \approx 1/\phi(a, v)$ corresponds to that portion of the line; it then follows that lg $\tau \approx 4.5$—5.0. The form of the H- and K-profiles in the region $\Delta\lambda = 0.30$ Å gives evidence in favour of the indicated depths being close to the region of the temperature minimum in the umbra. The source functions of both lines in this layer probably tend to the Planck function. Hence, the temperature in the region of the minimum is of the order of 3000—3500 K.

3. If no additional data are used, one should not give preference to either alternative of $\Delta\lambda_D$ and, consequently, one cannot make the true ratio S_K/S_H more precise. To solve this problem it is necessary to examine the centre-limb variation of the H- and K-profiles.

The authors wish to thank Mrs. I. P. Ischukova for writing the computer program.

References

BODE, G. (1965): Inst. Theor. Physik und Sternwarte Univ. Kiel.

BUMBA, V. (1960): Izv. Krym. Astrophys. Observ., *23*, 230.

ENGVOLD, O. (1967): Solar Phys., *2*, 234.

EFENDEVA, S. A. (1973): Issled. Geomagn. Aeron. Fiz. Soln., Irkutsk, *26*, 67.

GINGERICH, O., NOYES, R. W., KALKOFEN, W., and CUNY, Y. (1971): Solar Phys., *18*, 347.

HENOUX, J. C. (1969): Astron. Astrophys., *2*, 288.

HOUTGAST, J. (1970): Solar Phys., *15*, 273.

HOWARD, R. (1958): Astrophys. J., *127*, 108.

DE JAGER, C. and NEVEN, L. (1972): Solar Phys., *22*, 49.

KJELDSETH MOE, O. and MALTBY, P. (1969): Solar Phys., *8*, 275.

LINSKY, J. L. (1968): Smithsonian Special Report, No. 274.

LINSKY, J. L. (1970): Solar Phys., *11*, 355.

MATTIG, W. (1971): Solar Phys., *18*, 434.

MOORE, C. E., MINNAERT, M. G. J., and HOUTGAST, J. (1966): The Solar Spectrum 2935 A to 8770 Å, NBS Mouo, 61.

MUSTEL, E. R. and TSAP, T. T. (1960a): Izv. Krym. Astrophys. Observ., *22*, 75.

MUSTEL, E. R. and TSAP, T. T. (1960b): Izv. Krym. Astrophys. Observ., *23*, 299.

PACIOREK, J. (1965): Publ. Astron. Inst. Czech. Acad. Sci., No. 51, 69.

SHINE, R. A. and LINSKY, J. L. (1972): Solar Phys., *25*, 357.

SMITH van, E. P. (1960): Astrophys. J., *132*, 202.

STAVELAND, L. (1970): Solar Phys., *12*, 328.

STEPANOV, V. E. (1957a): Publ. Sternberg Astron. Inst., No. 100, 3.

STEPANOV, V. E. (1957b): Publ. Sternberg Astron. Inst., No. 100, 36.

TEPLITSKAYA, R. B. and EFENDEVA, S. A. (1971): Issled. Geomagn. Aeron. Fiz. Soln., Irkutsk, *20*, 143.

TEPLITSKAYA, R. B. and EFENDEVA, S. A. (1971): Soln. Dann., No. 3, 80.

TEPLITSKAYA, R. B. and EFENDEVA, S. A. (1973): Solar Phys., *28*, 369.

TROYAN, V. I. (1971): Astrometriya Astrofiz., *12*, 64.

WHITE, O. R. and SUEMOTO, Z. (1968): Solar Phys., *3*, 523.

WILSON, A. M. and WORRALL, G. (1969): Astron. Astrophys., *2*, 469.

WORRAL, G. and WILSON, A. M. (1969): Astron. Astrophys., *2*, 458.

ZWAAN, C. (1965): Rech. Astron. Observ. Utrecht, *17*, 4.